Electronic Supplementary Material (ESI) for ChemComm.
This journal is © The Royal Society of Chemistry 2019

Supporting Information

Fluorinated Carboxylic Acids as Powerful Building Blocks for the Formation of Bimolecular Monolayers

Harry Pinfold[1], Christopher Greenland[1], Graham Pattison‡[1] and Giovanni Costantini*[1]

1) Department of Chemistry, University of Warwick, Gibbet Hill Road, Coventry, CV4 7AL, UK.

‡) Present address: Chemistry Research Group, School of Pharmacy and Biomolecular Sciences, University of Brighton, Brighton, BN2 4GJ, UK.

Contents:

1. Experimental Details

Commercially available F4TPA (Fluorochem, 97%), TPA (Sigma, 98%), 2TPTZ (Fluorochem, 99%), 3TPTZ (Alfa Aesar, 97%) and heptanoic acid (Acros Organics, 98%) were used without further purification.

Preparation of 4TPTZ: A mixture of 4-cyanopyridine (1.0 g, 9.6 mmol), 18-crown-6 (0.1 g, 0.38 mmol) and potassium hydroxide (22.5 mg, 0.40 mmol) was dissolved in decalin (1.0 cm^3) and heated with stirring at 200 °C under nitrogen for 3 h. The solvent was evaporated under high vacuum to give a brown solid. This was washed with hot pyridine (3 x 5.0 cm^3) to leave white crystals, which were dissolved in 2.0 M hydrochloric acid (5.0 cm^3). Addition of aqueous ammonia led to the precipitation of a white solid which was filtered and dried under high vacuum; yield 0.65 g (65%). ^{1}H NMR (400 MHz, $CDCl_3$,) 8.56 (6 H, d, *J* = 5.6 Hz) and 8.94 (6 H, d, *J* = 5.6 Hz)

Saturated solutions of F4TPA and TPA were prepared via sonication and heating of an excess of the solid material in heptanoic acid. These solutions were left to settle for at least 24 hours after which time the saturated solution was separated from the remaining solid via filtration. Solutions of 2TPTZ and 3TPTZ were prepared at a concentration of 10^{-2} M by dissolving an appropriate amount of material in heptanoic acid. 4TPTZ was not soluble enough in heptanoic acid to make a 10^{-2} M solution, therefore saturated solutions of 4TPTZ were prepared in the same manner as was done for TPA and F4TPA. The mixed solutions used to form the bimolecular networks with F4TPA were prepared by mixing saturated F4TPA solution with 10^{-2} M 2TPTZ/10^{-2} M 3TPTZ/saturated 4TPTZ solution in a ratio of 1:9. In all three cases, precipitation of what were assumed to be bulk cocrystals/salt was observed to occur shortly after mixing the two solutions. Solution decanted from the cocrystals/salt was deposited onto a freshly cleaved HOPG (ZYB, TipsNano) surface. The bimolecular monolayers were observed at the interface between these solutions and the HOPG substrate. The bimolecular networks of TPA and 4TPTZ were prepared using the protocol reported by Kampschulte et al.[1], i.e., by deposition of a solution prepared by mixing saturated TPA and saturated 4TPTZ solution in a ratio of 1:1.

All STM measurements were performed under ambient conditions using a Veeco STM equipped with an A-type scanner head, coupled with a Nanoscope E controller. STM tips were prepared by cutting 0.25 mm 80/20 Pt/Ir wire (Goodfellow). Images were recorded in constant current mode, and the parameters used to obtain each image are given in the figure captions. The bias voltage was applied to the sample. All the presented STM images were Gaussian filtered. In order to obtain accurate unit cell dimensions, the effects of thermal drift were eliminated by using the underlying atomic lattice of the HOPG surface for calibration. This was achieved by changing the tunnelling parameters to values that resulted in atomic resolution of the underlying HOPG surface partway through recording an image of the molecular overlayer. The resulting images contain both atomic resolution of the substrate and molecular resolution of the overlayer. These images were then calibrated using the known dimensions of the atomic lattice of the HOPG surface (0.246 nm, hexagonal). The unit cell

dimensions given are the average values obtained from at least seven calibrated images acquired during different experiments. These accurately determined unit cell parameters were used to drift-correct the high-resolution STM images presented in the main text. STM images were analysed using WsXM[2] and LMAPper[3]. The proposed models were built using Avogadro[4]. The individual molecules used to build these models were geometry optimised using Gaussian03[5] at the 6-311G(d,p) level.

2. Self-Assembly Behaviour of the Carboxylic Acid Building Blocks

F4TPA

Solutions of F4TPA dissolved in heptanoic acid at concentrations ranging from saturated down to 10^{-5} M were tested. Despite multiple attempts, we never observed and evidence whatsoever that F4TPA self-assembles at the heptanoic acid/HOPG interface. Samples were scanned for multiple hours to ensure that any diffusion-limited self-assembly was given a chance to occur. We also made sure that both positive and negative bias voltages were tested as this has recently been shown to influence the self-assembly of carboxylic acids.[6]

TPA

Contrastingly, we were very readily able to observe the self-assembly of TPA at the heptanoic acid/HOPG interface. Deposition of a saturated solution of TPA leads to the formation of extended domains of the characteristic brickwork assembly of TPA (see Fig. S1 and Fig. S2).

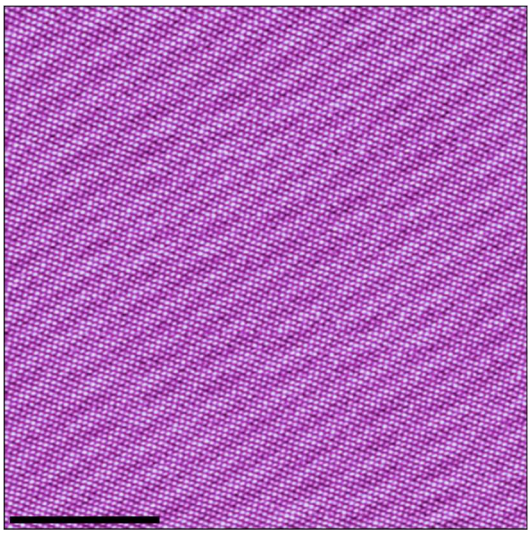

Fig. S1: Large-scale STM image showing the assembly of TPA at the heptanoic acid/HOPG interface. Tunnelling parameters: V_{bias} = −1.2 V, I_{set} = 300 pA. Scale bar = 20 nm.

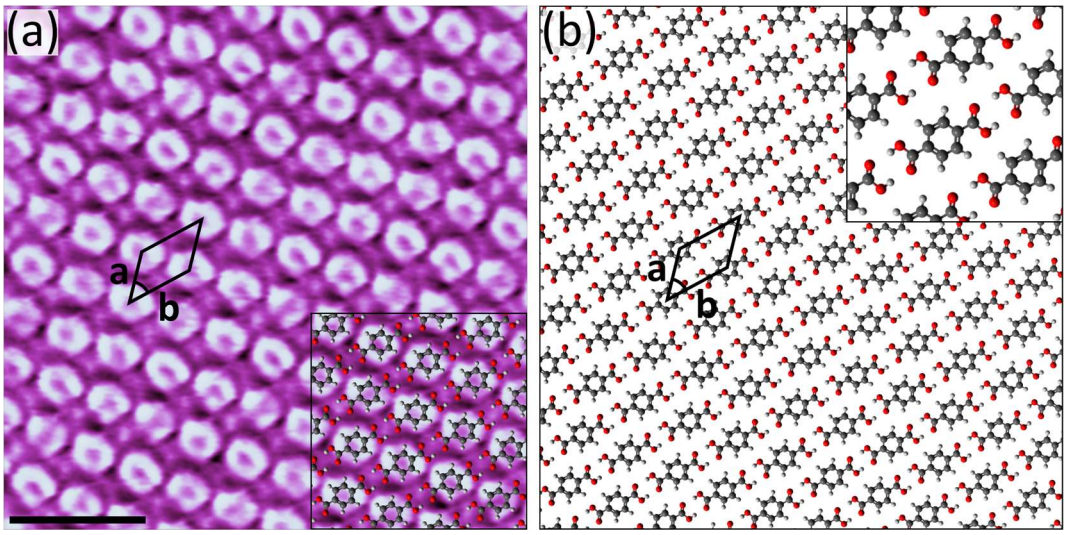

Fig. S2:(a) STM image showing the assembly of TPA at the heptanoic acid/HOPG interface. Tunnelling parameters: V_{bias} = −1.2 V, I_{set} = 200 pA. Unit cell parameters: a = 0.77 ± 0.05 nm, b = 1.0 ± 0.1 nm, angle 48 ± 3°. Scale bar = 2 nm. (b) Proposed model for the assembly.

3. Self-Assembly Behaviour of the Tripyridyltriazine Isomers

The self-assembly of 2TPTZ, 3TPTZ and 4TPTZ was studied at the heptanoic acid/HOPG interface in the absence of both TPA and F4TPA. Of the three isomers, only 4TPTZ was not observed to self-assemble under these conditions. There are contradictory reports in the literature regarding 4TPTZ: whilst Kampschulte et al. report that 4TPTZ does not self-assemble at the heptanoic acid/HOPG interface[1], Li et al. suggest that it does[7]. We tested solutions with concentrations ranging from saturated down to 10^{-5} M and did not observe any evidence that 4TPTZ self-assembles at the heptanoic acid/HOPG interface.

2TPTZ

Deposition of a 10^{-2} M solution of 2TPTZ dissolved in heptanoic acid results in the formation of an approximately hexagonal array at the heptanoic acid/HOPG interface (see Fig. S3). The assembly has two equivalent unit cell vectors with lengths of 2.5 ± 0.2 nm, separated by an angle of 60 ± 3°. In high-resolution STM images, such as that presented in Fig. S4, the 2TPTZ molecules can be clearly resolved. These 2TPTZ molecules are not closely packed, and there are no obvious strong interactions between them. Although it cannot be clearly resolved, there does appear to be some structure within the hexagonal pores defined by the 2TPTZ molecules. We expect that coadsorbed heptanoic acid molecules interacting with the 2TPTZ molecules via O−H···N(pyridyl) hydrogen bonds are likely present within these regions and that these solvent molecules are significant in stabilising the assembly.

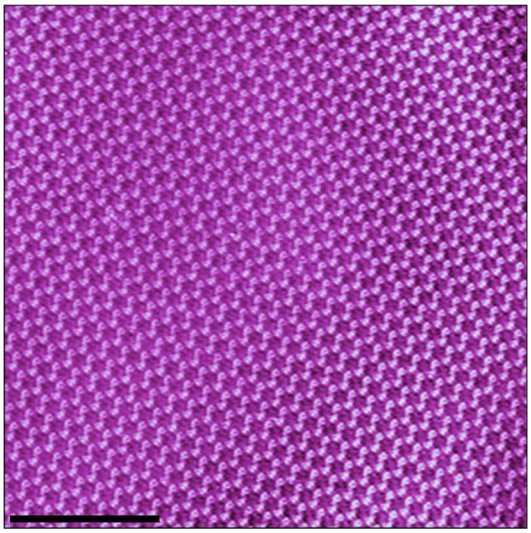

Fig. S3: Large-scale STM image showing the assembly of 2TPTZ at the heptanoic acid/HOPG interface. Tunnelling parameters: V_{bias} = −0.9 V, I_{set} = 100 pA. Scale bar = 20 nm.

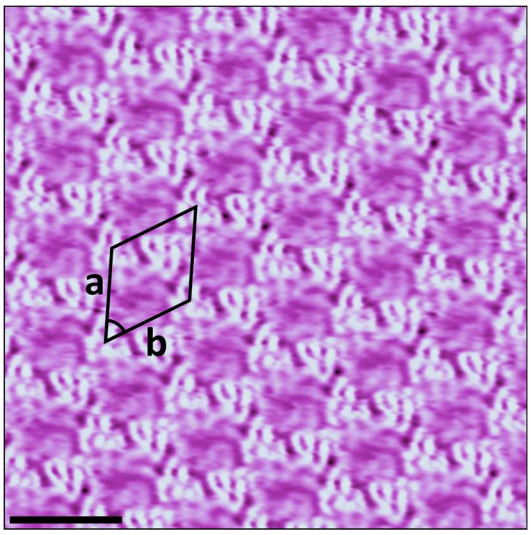

Fig. S4: STM image showing the assembly of 2TPTZ at the heptanoic acid/HOPG interface. Tunnelling parameters: V_{bias} = −1.5 V, I_{set} = 50 pA. Unit cell parameters: a = b = 2.5 ± 0.2 nm, angle 60 ± 3°. Scale bar = 3 nm.

We also investigated how the concentration of 2TPTZ influences the assembly. Concentrations ranging from 10^{-5} – 10^{-2} M were tested. No evidence of any concentration-dependent polymorphism was observed within this range. The hexagonal assembly of 2TPTZ could be observed covering essentially the entire surface of the sample at concentrations of 10^{-2} M, 10^{-3} M and 5×10^{-4} M. At a concentration of 2.5×10^{-4} M occasional domains of the hexagonal assembly of 2TPTZ could be observed, but the assembly was absent from most of the surface. For all of the concentrations below 2.5×10^{-4} M that were sampled, no evidence of any assembly was observed. These observations are summarised in Fig. S5.

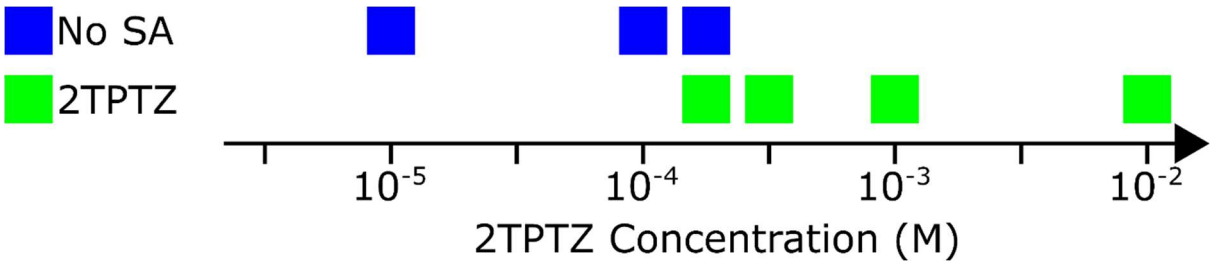

Fig. S5: Profile showing the different observations made at the heptanoic acid/HOPG interface as the concentration of 2TPTZ is changed. Blue squares indicate that no assembly is present at the interface. Green squares indicate that the hexagonal assembly of 2TPTZ is present.

3TPTZ

Deposition of a solution of 3TPTZ dissolved in heptanoic acid at a concentration of 10^{-2} M leads to the formation of a self-assembled monolayer at the heptanoic acid/HOPG interface (see Fig. S6). The approximately hexagonal assembly has two equivalent lattice vectors with lengths of 3.5 ± 0.3 nm separated by an angle of 60 ± 3°. The threefold symmetric 3TPTZ molecules can be readily resolved in high-resolution STM images such as that presented in Fig. S7a. These molecules are positioned such that they can interact with one another via C–H···N(pyridyl) non-classical hydrogen bonds. These interactions organise the 3TPTZ molecules into cyclic structures, each of which is composed of six 3TPTZ molecules. The pyridyl nitrogen atoms on the periphery of the cyclic structures are not positioned such that they can interact with neighbouring 3TPTZ molecules. We expect that these free pyridyl nitrogen atoms likely interact with coadsorbed solvent molecules via O–H···N(pyridyl) interactions as such hydrogen bonds are quite favourable and heptanoic acid molecules can be readily incorporated into the space between the cyclic structures. Note that the proposed coadsorbed heptanoic acid molecules cannot be clearly resolved. A tentatively proposed model is given in Fig. S7b.

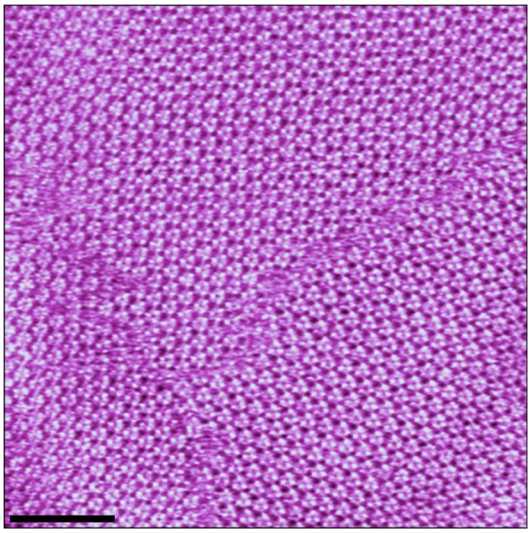

Fig. S6: Large-scale STM image showing the assembly of 3TPTZ at the heptanoic acid/HOPG interface. Tunnelling parameters: V_{bias} = −0.9 V, I_{set} = 100 pA. Scale bar = 20 nm.

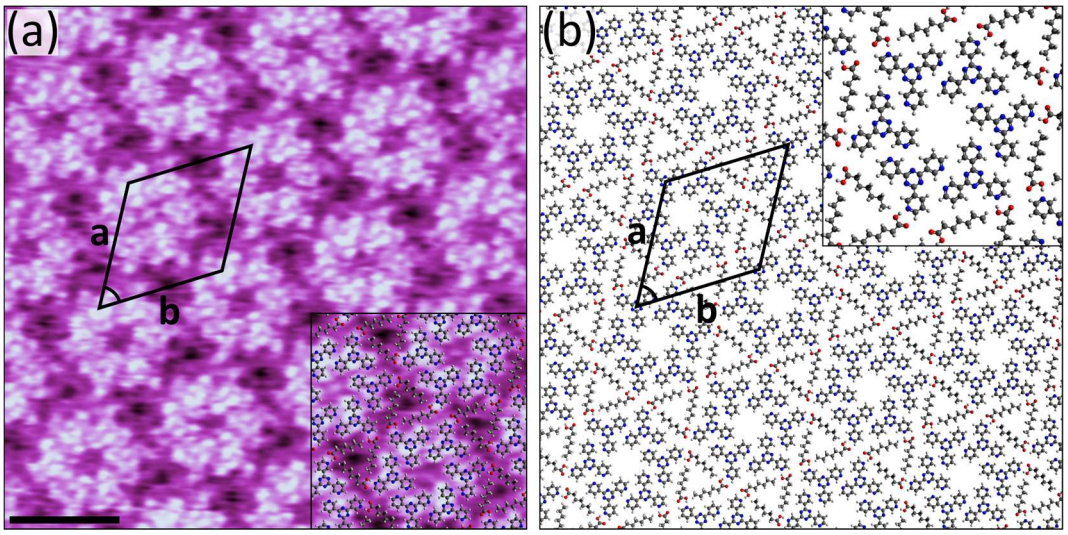

Fig. S7: (a) STM image showing the assembly of 3TPTZ with coadsorbed solvent molecules at the heptanoic acid/HOPG interface. Tunnelling parameters: V_{bias} = −0.9 V, I_{set} = 100 pA. Unit cell parameters: a = b = 3.5 ± 0.3 nm, angle 60 ± 3°. Scale bar = 3 nm. (b) Proposed model for the assembly.

We also investigated the influence of the concentration on the self-assembly of 3TPTZ. As is summarised in Fig. S8, the hexagonal assembly of 3TPTZ could be observed covering essentially the entire surface of the sample at concentrations ranging from $2.5 \times 10^{-3} – 10^{-2}$ M. At concentrations of 10^{-3} M and below, no assembly could be observed.

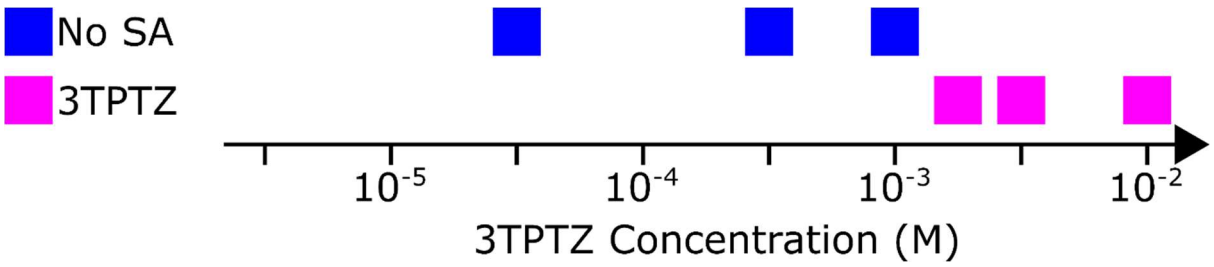

Fig. S8: Profile showing the different observations made at the heptanoic acid/HOPG interface as the concentration of 3TPTZ is changed. Blue squares indicate that no assembly is present at the interface. Pink squares indicate that the hexagonal assembly of 3TPTZ is present.

4. Attempts to Fabricate Bimolecular Networks using TPA and 2TPTZ/3TPTZ

2TPTZ and TPA

We started by trying to fabricate bimolecular networks by pairing 2TPTZ with TPA. Solutions containing these two molecules were prepared at a range of compositions as the formation of bimolecular networks could depend on this parameter. The concentration of TPA in all solutions was saturated whilst the concentration of 2TPTZ was varied. These solutions were deposited onto HOPG substrates and imaged via STM. Experiments were conducted in exactly the same manner as those performed with F4TPA. The only ordered networks we ever observed were those corresponding to either pure 2TPTZ or pure TPA. These results are summarised in Fig. S9. Each point in this figure is the result of analysing at least five distinct ~0.5 μm^2 regions of a freshly prepared samples surface.

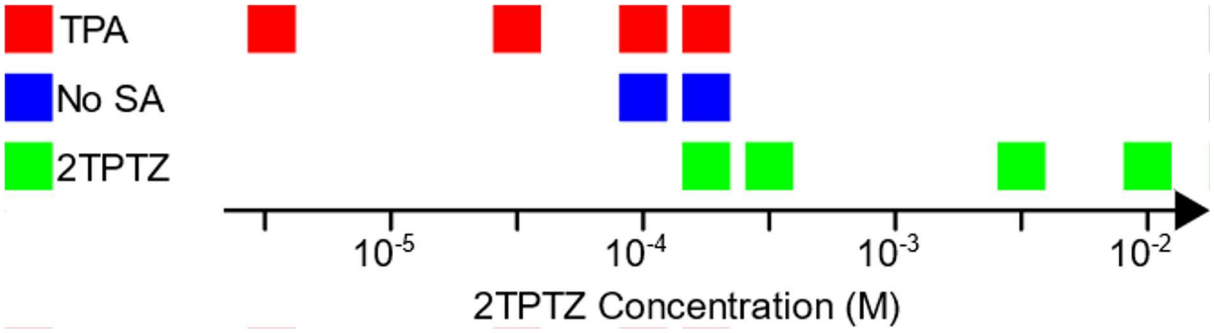

Fig. S9: Profile showing the different observations made at the heptanoic acid/HOPG interface as the concentration of 2TPTZ is changed in a saturated solution of TPA. Red squares indicate that the homomolecular assembly of TPA (see section 2) was observed, green squares indicate that the hexagonal assembly of 2TPTZ (see section 3) was observed and blue squares indicate that no assembly could be observed. A description of what was observed at each concentration is given below.

- **10^{-2} – 5×10^{-4} M**: The hexagonal assembly of pure 2TPTZ could be observed covering essentially the entire surface of the sample.
- **2.5×10^{-4} M**: Both the homomolecular assembly of TPA and the hexagonal assembly of 2TPTZ were observed coexisting on the surface. Immediately after depositing, assembly was not present on an appreciable amount of the surface, but over the course of a few hours the assemblies of TPA and 2TPTZ began to dominate.
- **10^{-4} M**: Large domains of the pure TPA assembly could be frequently encountered, but assembly was absent from much of the surface.
- **5×10^{-5} – 5×10^{-6} M**: The homomolecular assembly of TPA could be observed covering essentially the entire surface of the sample.

At high relative concentrations of TPA, the homomolecular assembly of this molecule dominates. As the relative concentration of 2TPTZ in the solution is increased, the assembly corresponding to pure 2TPTZ begins to take over. At the transition between the assemblies of TPA and 2TPTZ we also began to see regions of the surface on which no assembly appeared to be present. The most significant observations were those obtained when the concentration of 2TPTZ was 2.5×10^{-4} M. At this composition we were able to observe the homomolecular assembly of TPA and the hexagonal assembly of 2TPTZ coexisting on the surface. Typically, the domains of 2TPTZ were separated from the homomolecular domains of TPA by steps/defects in the HOPG surface. However, as is shown in Fig. S10, we did occasionally observe domains directly interfacing with one another. The fact that phase-separated domains of 2TPTZ and TPA could be observed is strong evidence that these two molecules are not inclined towards coassembly.

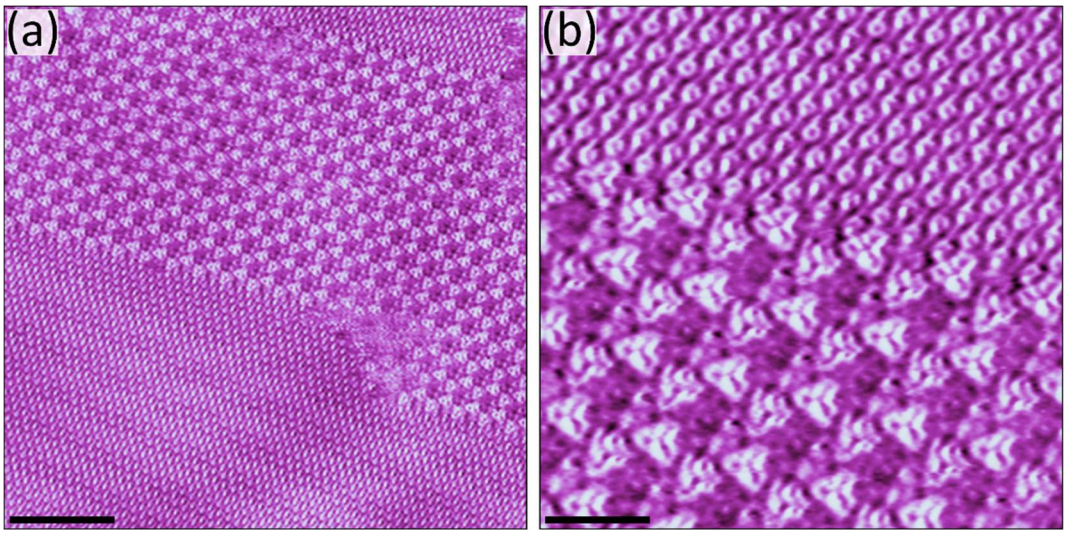

Fig. S10: (a) STM image showing phase-separated domains of 2TPTZ and TPA at the heptanoic acid/HOPG interface. Tunnelling parameters: V_{bias} = −0.9 V, I_{set} = 50 pA. Scale bar = 10 nm. (b) STM image showing the interface between the phase-separated domains. Tunnelling parameters: V_{bias} = −0.9 V, I_{set} = 50 pA. Scale bar = 3 nm.

3TPTZ and TPA

A comparable series of experiments was also performed with solutions containing both 3PTTZ and TPA. The results of these experiments are summarised in Fig. S11. In this case, we also observed the homolecular self-assembly of TPA when the concentration of 3TPTZ in the solution was relatively low. At higher concentrations of 3TPTZ we were able to observe its hexagonal assembly covering essentially the entire surface of the sample. At intermediate 3TPTZ concentrations we observed significant areas of the surface on which there was no evidence of any self-assembled structures. We did not observe the coexistence of both assemblies under any of the tested conditions. No indication whatsoever of 3TPTZ and TPA forming a bimolecular network was observed with any of the solution compositions.

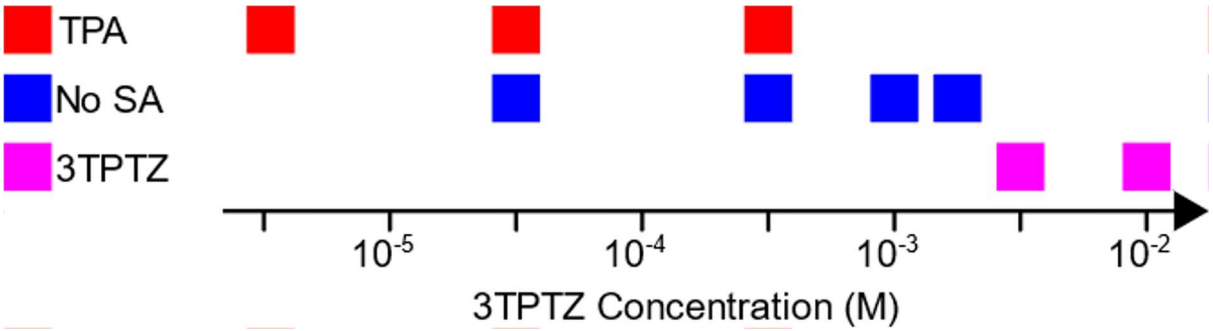

Fig. S11: Profile showing the different observations made at the heptanoic acid/HOPG interface as the concentration of 3TPTZ is changed in a saturated solution of TPA. Red squares indicate that the homomolecular assembly of TPA (see section 2) was observed, pink squares indicate that the hexagonal assembly of 3TPTZ (see section 3) was observed and blue squares indicate that no assembly could be observed. A description of what was observed at each concentration is given below.

10^{-2} – 5 × 10^{-3} M: The hexagonal assembly of pure 3TPTZ could be observed covering essentially the entire surface of the sample.

2.5 × 10^{-3} – 10^{-3} M: No assembly could be observed on the surface of the sample.

5 × 10^{-4} M: There was no assembly present on the vast majority of the surface, but occasional isolated domains of the homomolecular assembly of TPA could be encountered.

5 × 10^{-5} M: The homomolecular assembly of TPA could be observed covering most of the surface of the sample, but occasional regions in which no self-assembly could be observed were also present.

5 × 10^{-6} M: The homomolecular assembly of TPA could be observed covering essentially the entire surface of the sample.

Although the formation of bimolecular networks could not be observed, 3TPTZ and TPA do seem to interfere with one another's homomolecular assembly to some extent. In the absence of TPA, 3TPTZ self-assembles into its expected hexagonal network at a concentration of 2.5 × 10^{-3} M (see Fig. S8). However, at the same concentration in the solution containing TPA no assembly could be observed (see Fig. S11). This indicates that the presence of TPA disrupts the formation of the hexagonal network at this concentration. Furthermore, the concentration of TPA in the solutions is sufficiently high that full surface coverage could be expected; however, at concentrations ranging from 2.5 × 10^{-3} – 5 × 10^{-5} M the homomolecular assembly of TPA is either not observed or the extent to which it covers the surface is reduced. This indicates that the presence of 3TPTZ also disrupts the homomolecular assembly of TPA.

5. Conformations of 2TPTZ and 3TPTZ

2TPTZ

As is shown in Fig. S12, 2TPTZ can adopt two distinct planar conformations. One of the two configurations is threefold-symmetric as all the pyridyl rings are orientated in the same direction (Fig. S12a). In the alternate configuration, one of the pyridyl rings is orientated in the opposite direction relative to the other two (Fig. S12b). Simple DFT calculations were employed to evaluate the relative stability of the two possible conformations. These calculations were performed for isolated gas-phase molecules at the B3LYP/6-311g(d,p) level using Gaussisan03[5]. The threefold-symmetric conformation was found to be 12.2 kJ/mol more stable than the alternate conformation. As this value is approximately five times larger than thermal energy at room temperature, we expect that the threefold-symmetric conformation of 2TPTZ is present in the assembly. This result is consistent with previous studies.[8]

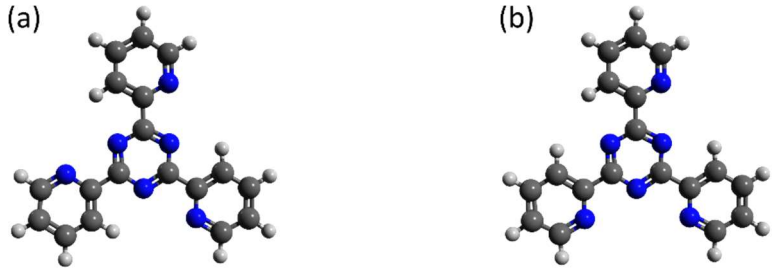

Fig. S12: (a) Threefold-symmetric conformation of 2TPTZ. (b) Alternate configuration of 2TPTZ.

3TPTZ

3TPTZ can also adopt two different planar conformations in the same manner as 2TPTZ, i.e., a threefold-symmetric configuration in which all the pyridyl groups are orientated in the same direction (Fig. S13a) and an alternate configuration in which one of the pyridyl rings is flipped (Fig. S13b). In this case, the threefold-symmetric conformation was found to be only 0.9 kJ/mol more stable than the alternate conformation. As this value is smaller than thermal energy at room temperature, we expect that either configuration is possible under the experimental conditions. In the bimolecular network formed between 3TPTZ and F4TPA, the 3TPTZ molecules must adopt the non-threefold-symmetric configuration in order to maximise the number of strong hydrogen bonds.

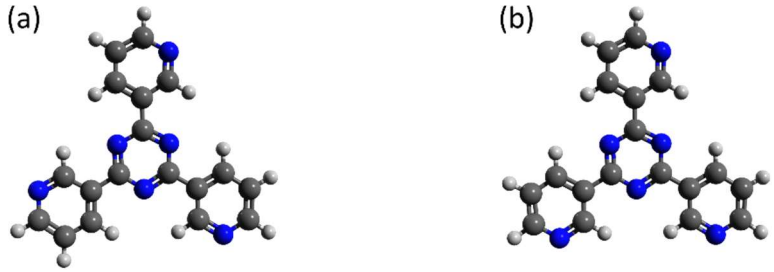

Fig. S13: (a) Threefold-symmetric conformation of 3TPTZ. (b) Alternate configuration of 3TPTZ.

6. Large-Scale STM Images of the Bimolecular Networks

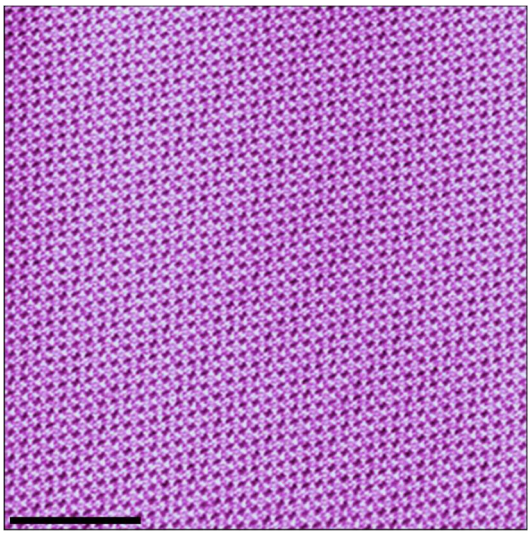

Fig. S14: Large-scale STM image showing the bimolecular assembly of TPA and 4TPTZ at the heptanoic acid/HOPG interface. Tunnelling parameters: V_{bias} = −1.2 V, I_{set} = 70 pA. Scale bar = 20 nm.

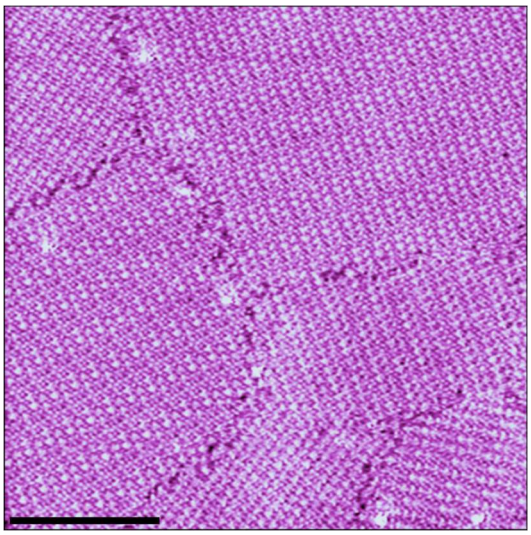

Fig. S15: Large-scale STM image showing the bimolecular assembly of F4TPA and 2TPTZ at the heptanoic acid/HOPG interface. Multiple domains are present. Tunnelling parameters: V_{bias} = −0.9 V, I_{set} = 50 pA. Scale bar = 20 nm. This assembly has a very characteristic moiré pattern that appears as a modulation in the contrast occurring periodically every four lattice spacings along the direction of the short lattice vector (a in Fig. 3a in the main text). This effect can be clearly observed in Fig. S15 and in Fig. 3a.

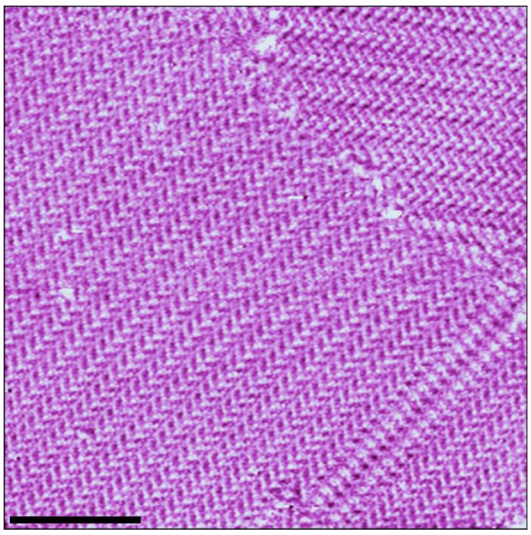

Fig. S16: Large-scale STM image showing the bimolecular assembly of F4TPA and 3TPTZ at the heptanoic acid/HOPG interface. Multiple domains are present. Tunnelling parameters: V_{bias} = −1.2 V, I_{set} = 100 pA. Scale bar = 20 nm.

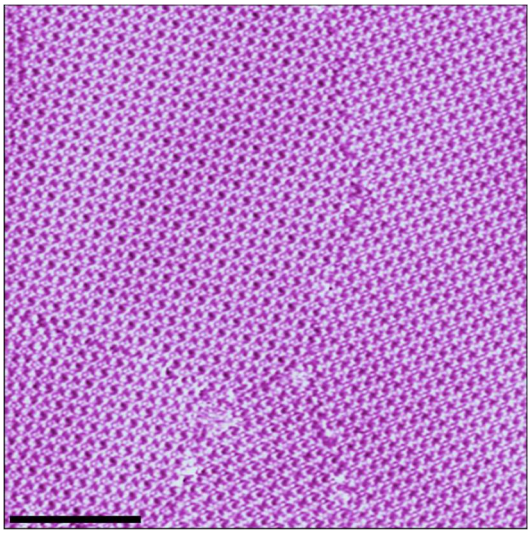

Fig. S17: Large-scale STM image showing the bimolecular assembly of FTPA and 4TPTZ at the heptanoic acid/HOPG interface. Multiple domains are present. Tunnelling parameters: V_{bias} = −1.1 V, I_{set} = 70 pA. Scale bar = 20 nm.

7. References

1 L. Kampschulte, S. Griessl, W. M. Heckl and M. Lackinger, *J. Phys. Chem. B*, 2005, **109**, 14074–14078.

2 I. Horcas, R. Fernández, J. M. Gómez-Rodríguez, J. Colchero, J. Gómez-Herrero and A. M. Baro, *Rev. Sci. Instrum.*, 2007, **78**, 013705.

3 LMAPper - The SPM and Mol Viewer, https://sourceforge.net/projects/spm-and-mol-viewer/, (accessed 1 August 2019).

4 M. D. Hanwell, D. E. Curtis, D. C. Lonie, T. Vandermeersch, E. Zurek and G. R. Hutchison, *J. Cheminformatics*, 2012, **4**, 17.

5 M. Frisch, G. Trucks, H. Schlegel, G. Scuseria, M. Robb, J. Cheeseman, J. Montgomery, T. Vreven, K. Kudin, J. Burant, J. Millam, S. Iyengar, J. Tomasi, V. Barone, B. Mennucci, M. Cossi, G. Scalmani, N. Rega, G. Petersson, H. Nakatsuji, M. Hada, M. Ehara, K. Toyota, R. Fukuda, J. Hasegawa, M. Ishida, T. Nakajima, Y. Honda, O. Kitao, H. Nakai, M. Klene, X. Li, J. Knox, H. Hratchian, J. Cross, V. Bakken, C. Adamo, J. Jaramillo, R. Gomperts, R. Stratmann, O. Yazyev, A. Austin, R. Cammi, C. Pomelli, J. Ochterski, P. Ayala, K. Morokuma, G. Voth, P. Salvador, J. Dannenberg, V. Zakrzewski, S. Dapprich, A. Daniels, M. Strain, O. Farkas, D. Malick, A. Rabuck, K. Raghavachari, J. Foresman, J. Ortiz, Q. Cui, A. Baboul, S. Clifford, J. Cioslowski, B. Stefanov, G. Liu, A. Liashenko, P. Piskorz, I. Komaromi, R. Martin, D. Fox, T. Keith, A. Laham, C. Peng, A. Nanayakkara, M. Challacombe, P. Gill, B. Johnson, W. Chen, M. Wong, C. Gonzalez and J. Pople, *Gaussian 03, Revision C.02*, 2003.

6 F. P. Cometto, K. Kern and M. Lingenfelder, *ACS Nano*, 2015, **9**, 5544–5550.

7 M. Li, P. Xie, K. Deng, Y.-L. Yang, S.-B. Lei, Z.-Q. Wei, Q.-D. Zeng and C. Wang, *Phys. Chem. Chem. Phys.*, 2014, **16**, 8778–8782.

8 J. Janczak, M. Śledź and R. Kubiak, *J. Mol. Struct.*, 2003, **659**, 71–79.